MATHEMATICAL MODELS OF CONFINEMENT AND DECONFINEMENT

Satyanad Kichenassamy

MATHEMATICAL MODELS OF CONFINEMENT AND DECONFINEMENT

SATYANAD KICHENASSAMY

Abstract. We propose a class of confinement and deconfinement strategies based on new space-extended SIR models that model confinement of part of the population as well as their partial mobility. Our model differs from earlier ones by the introduction of a term reflecting government-induced restrictions on travel between regions. It is shown that a deconfinement procedure that preferentially allows communication between regions with a similar infection rate can stall the growth of the epidemic in the less infected regions, while avoiding complete lockdown. We also propose to introduce a new set of compartments for confined susceptibles and infectives. The model is compared to exisiting models.

Background. Mobility in SIR models has so far only taken into account the structural factors and behavior patterns that limit or encourage mobility, but not the possibility of nationwide government action based on a real-time estimation of the sanitary situation in individual regions.

Method. We modify a space-extended SIR model by the introduction of a limitation on travel between regions in which the sanitary situation is significantly different. Compartments represent urban centers, connected to others by rail, air or highways. We also include new compartments for partially confined individuals, whether infectives or not. Mobility may take into account region attractivity, government action, and citizens' rational decisions in response to them.

Findings. The proposed modification prevents all regions from reaching their peak at the same time, while allowing some communication between them. It seems realistic to implement a deconfinement policy in which the interregional restrictions would be based on the relative difference in infection rates rather than the absolute infection rate of a region, or on interregional distance.

Recommendations. During deconfinement, travel restrictions should be based on the difference of the epidemic level between regions, rather than distance, or the absolute epidemic level. For instance, if the regions of the country are classified as "red" or "green" zones, there should be fewer restrictions for travel between red regions that between red and green regions.

Keywords: Covid-19, SARS-Cov-2, SIR model, confinement and deconfinement, lockdown.

1. Introduction

Confinement measures have stalled the Covid-19 epidemic, but did not quell it. It is therefore necessary to devise a procedure for deconfinement that limits the number of new cases it will necessarily induce. We propose a strategy that, in a somewhat

Date: version 2: 3 mai 2020.

counter-intuitive fashion, both allows a measure of population mobility and prevents all regions from reaching a peak of infection at the same time.

The compartmental approach has been used for about a century for modeling epidemics, and has been adapted to the recent situation. Its space-extended versions are appropriate in countries in which mobility mostly consists of travel between urban centers (called "regions" in the sequel), through public transportation or highways. We introduce here two new elements. This proposal takes stock of the current consensus in epidemiology, and seeks to introduce spatial variation without losing the advantages of the compartmental approach. Indeed, the SIR model and its variants,[1] by summarizing spatial interaction in the mass-action term, can only be modified into a space-dependent setup in two ways: by modifying the mechanism of interaction, and by introducing different compartments for different regions. It follows from a recent survey of spatially-extended TSIR models (Bjørnstad, Grenfell, Viboud and King, 2019) that all earlier approaches amount to replacing terms of the form $\beta SI/N$ in the usual equations by $\beta S(I+\iota)/N$,[2] where ι depends on the model. We propose here to incorporate into ι a factor representing government-imposed restrictions on travel between regions, on top of a model for population mobility and show its effect on a example. For other metapopulation approaches, see e.g. [6, 1], and their references. It seems that none of these approaches has incorporated governement-imposed restrictions on mobility that depend on the infection levels in the various regions. Indeed, the possibility of dynamically controlling the means of transmission of the epidemic by government action, on the basis of a real-time estimation of metapopulations through tracking and testing, is an unprecedented development, that makes the deconfinement strategy proposed here realistic.

In this paper, confinement and deconfinement are modeled at two levels. At the inter-regional level, we propose to limit the allowed flux of population in terms of the gradient of a measure of the sanitary situation of the individual regions, and obtain easily implementable, government-induced restrictions on travel that propose a compromise between mobility and safety. While many works have proposed models of population movement during the spread of an epidemic, it seems that none have incorporated the effect of such nationwide measures, that are indeed unprecedented. We show on examples that this has the effect of preventing less-infected regions from reaching a peak at the same time as the others. In some cases, a plateau rather than a peak is observed. Note that nation-wide measures not only affect the physical possibilities for travel, but also modifies the actors' rational choices by providing public information about the epidemic in real time. At the intra-regional level, the effects of confinement measures are modeled by the time variation of the reproduction rate. Our second new element is the introduction of subcompartments within the compartments of susceptible and infective, that seem to represent more faithfully than other models the actual situation of lockdown.

Regarding the choice of the movement model, it seems that a "simple-trip" model with a well-defined home location (as in Citron et al., 2020) reflects the situation in France. That is why we did not allow for migration (for extended holidays for instance). The implicit assumption that the infectious periods are exponentially distributed could be removed by introducing further compartments, as was shown by Keeling and Grenfell (2001) and Lloyd (2002).

[1] Kermack and McKendrick (1927). Since we are dealing with short periods, we neglect births. Age-related transmission could be also included in the obvious manner.

[2] Or more generally, $\beta S(I+\iota)^\alpha/N$. The extension of our considerations to this case is immediate.

1.1. **New elements in our model.** In (Bjørnstad et al., 2019), the number I_j of infectious persons in region A_j that occurs in the "mass-action" terms is replaced by an expression of the form $I_j + \iota_j$ where $\iota_j = \sum_{i \neq j} \psi_{ij}(I_k) I_i$. We modify it by taking $\iota_j = \sum_{i \neq j} m_{ij}(t) \psi_{ij}(I_k)(1 + [I_i/N_i - I_j/N_j]^2/K^2)^{-1}$. For earlier models, see Bjørnstad et al. (2019), or Arenas et al. (2020) [1] and their references.

We construct our models by successive generalizations, starting from a standard SIR model, spelling out the meaning of the assumptions introduced at each step. We first deal with the gradual reinstatement of communication between regions, and then deal with the issue of intraregional deconfinement by introducing subcompartments to deal with confined classes[3]. Other recent proposals include (Wu et al. (2020) and Sardar (2020) and Nadim et al. (2020); the latter propose seven compartments (susceptibles, exposed, quarantined, asymptomatic, symptomatic, isolated and recovered individuals) see . By contrast, in the present model, confined individuals are not quarantined, and could be susceptible as well as infective (or recovered). Our proposal represents more faithfully the current situation, by the structure of its compartments, and also by recognizing the nonzero mobility of confined classes.

1.2. **Possible extensions and variants.** On the relation between deterministic and probabilistic compartmental models, see e.g. Keeling and Ross (2007). For the estimation of the reproduction rate in various mobility models, see [2].

In a different direction, one could include a finer game-theoretic analysis of social distancing [3], that takes into account the cost of infection for the individual, this cost being modeled as an increasing function of the current infection rate. This would amount to introducing a dependence on I_j in some of the β coefficients. The present model could be modified along these lines.

We assume that the effect of intra-regional confinement is the reducion of the effective value β_i of β in each region, by decreasing the possibility of contact between susceptibles and infectives. Another approach is to consider that confinement reduces the number of susceptibles, while keeping β constant, by assuming that the population of susceptibles and asymptomatic infectives are depleted at a constant rate, at the expense of a quarantined compartment (Maier and Brockmann, 2020). However, their paper deals with the early phase of the epidemic. By contrast, we are interested here in the deconfinement period, to that the assumption of constant-rate depletion does not seem appropriate.

2. Communication between regions

2.1. **A model for each region.** Consider first a spatially extended SIR model with several regions A_i, in which there are S_i susceptibles, I_i infectives and R_i recovered. With obvious notation, if there is no interaction between regions, the unknowns satisfy (primes denote time derivatives)

$$S_i' = -\beta_i S_i I_i / N_i \tag{1}$$

$$I_i' = \beta_i S_i I_i / N_i - (\gamma + d) I_i \tag{2}$$

$$R_i' = \gamma I_i. \tag{3}$$

[3]With sufficient computing power, it would be possible to subsume the second issue under the first, treating each home as a different "region," but this would require to take into account the qualitative differences between communication between urban centers and communication within a city.

The coefficients β_i could depend on time. Indeed, if confinement is successful, we expect $R_{0i} := \beta_i/\gamma$ to decrease. Here, we have assumed that the recovery rate and the death rate are the same for all regions – which is reasonable if the health system is the same throughout the country.

2.2. **Introduction of communication between regions: Models A and B.** Let us now assume that the susceptibles can be infected by contact with infectious individuals from other regions:

$$S_i' = -\beta_i S_i \left(I_i + \iota_i\right)/N_i \tag{4}$$

$$I_i' = \beta_i S_i \left(I_i + \iota_i\right)/N_i - (\gamma + d) I_i \tag{5}$$

$$R_i' = \gamma I_i, \tag{6}$$

with

$$\iota_i = \sum_{j \neq i} M_{ij} I_j, \tag{7}$$

$$M_{ij} = \frac{m_{ij}\varphi_{ij}}{1 + D_{ij}^2/K^2}, \tag{8}$$

$$D_{ij} = I_i/N_i - I_j/N_j, \tag{9}$$

where the parameters m_{ij} and K define the deconfinement strategy, and N_i is the total population of region A_i, while φ_{ij} represent the fraction of the infectives in region A_j that could enter in contact with susceptibles in A_i, because of commuting, or family or shopping trips. Thus, m_{ij} and K represent government action, based on a detailed knowledge of the situation in all regions, while φ_{ij} models the mobility that individuals would have under normal circumstances. This model is therefore well-adapted to a gradual deconfinement situation. Assumptions are as follows:

- individuals try and return to their normal mobility patterns, based only on local knowledge of the situation, and the synthetic information provided by the media;
- government action acts the basis of global information, directly on m_{ij} and K through restrictions on interregional travel, and indirectly on the β_i through more or less stringent confinement rules within each region.

It follows that government action has three different dimensions: it reduces inter-regional travel, it reduces intra-regional mobility and it acts on peoples' judgement by making information publicly available.

Note that $0 \leq M_{ij} \leq m_{ij}\varphi_{ij}$, and that the second inequality becomes an equality when the infection rates in the two regions are equal. Limiting cases are as follows.

- If K is very large, the M_{ij} are very close to $m_{ij}\varphi_{ij}$. If in addition all the $m_{ij} = 1$, the S_i susceptibles interact with all the infected as they used to in pre-epidemic conditions. This represents the stage of full deconfinement.
- If on the contrary all the $m_{ij} = 0$, the value of K becomes irrelevant, and in this situation, all regions boundaries are closed.
- To encourage communication between A_i and A_j is to make M_{ij} closer to φ_{ij}, by increasing m_{ij} or K.
- A larger value of K means that the mobility is *less* dependent on the infection levels of the regions. Conversely, a very small K means that the model is *very sensitive* to differences in infection levels.

The restriction on inter-regional travel depends on a measure D_{ij} of the difference in the sanitary situation in the two regions involved. We have taken D_{ij} to depend on the infection levels. It would be possible to include a more complex indicator that takes into account the number of available intensive care units (ICU) in the target regions.[4]

We propose two possible methods for the choice of φ_{ij} — the fraction of infectives in one region that can interact with susceptibles of the other: either by estimating them on the basis of normal behavior patterns, or on the basis of subjective reactions to information about this exceptional situation, that is broadcast by the government. We distinguish two approaches.

In *Model A*, we take for $\varphi_{ij} = \varphi_{ij}^A$ the value of ι_{ij} given by one of the models described by Brønstad et al.. As they explain, there seem to be two main strategies for modeling mobility in the absence of disease: the "gravity" model, and variants of Stouffer's model. In the former, the attractivity of travel from region A_i to region A_j is inversely proportional to some power of the distance d_{ij} between them, hence the name. In the latter, regions A_k that are closer to A_i than to A_j are taken into account, considering that they provide "opportunities" that compete with A_j for preferential travel to it. Both models include a multiplicative parameter θ (or two parameters θ and ϕ, see [4]). Our proposal to replace φ_{ij} by M_{ij} amounts to making these parameters depend on the difference between the infection levels in the two regions involved.

A slightly more detailed analysis of the infection process (Pei and Shaman (2020)) distinguishes between daytime and nighttime transmission.

Model B assumes that individuals modify their normal behavior patterns by exercising their judgement, on the basis of public information. We therefore propose to let $\varphi_{ij} = \varphi_{ij}^B$, where φ_{ij}^B represents the mobility that a typical individual in A_j might consider rational given the current information about the level of infection and the possible saturation of the ICU. This decision in turn also depends on government-controlled information. For instance, assume that there are B_j^{av} available ICU units out of a total of B_j in region A_j, and that a typical citizen is aware of this. Obviously, if $B_j^{av} = B_j$, a rational actor would be reluctant to travel to region A_j. Therefore, the coefficient representing the tendency to move from A_j to A_i would have the form $\varphi_{ij}^B = S(B_j^{av}/B_j - B_i^{av}/B_i)$ where S is a nonnegative sigmoid function on $[-1, 1]$. Thus, travelers would be reluctant to travel if $B_j^{av}/B_j \ll B_i^{av}/B_i$.

Hybrid models combining features of Model A and Model B are also possible.

2.3. **An example.** As a simple illustration that the suggested mechanism actually has the expected consequences, let us consider the case of three regions A_1, A_2 and A_3, in which the rates of infection are initially 20%, 2% and 10% respectively. We take $\gamma = 1$, $d = 0.1$; β is the same in all three regions, and varies with the simulation. We assume that regions A_2 and A_3 interact only with A_1 ($m_{23} = 0$).

All figures describe the time evolution of the proportions of infected patients I_i/N_i for various choices of parameters. in Figures 1-5, $\beta = 3$; in Fig. 6, $\beta = 1.6$; in Fig. 7, $\beta = \frac{t}{8} \times 0.6 + (1 - \frac{t}{8}) \times 1.6$ ($t \in [0, 8]$) and in Fig. 7, $\beta = \frac{t}{8} \times 0.8 + (1 - \frac{t}{8}) \times 3$ ($t \in [0, 8]$).

Figure 1 describes the situation where the regions are disconnected. There are three distinct infection peaks, reflecting the differences in initial infection levels.

[4]For instance, $D_{ij} = |I_i/N_i - I_j/N_j| + \alpha(L_i)+$, where L_j is the number of available ICU units in region A_j, and α is decreasing. Thus, the smaller the value of L_i, the stronger restriction on travel into A_i. Another implementation of the same idea is proposed in Model B below.

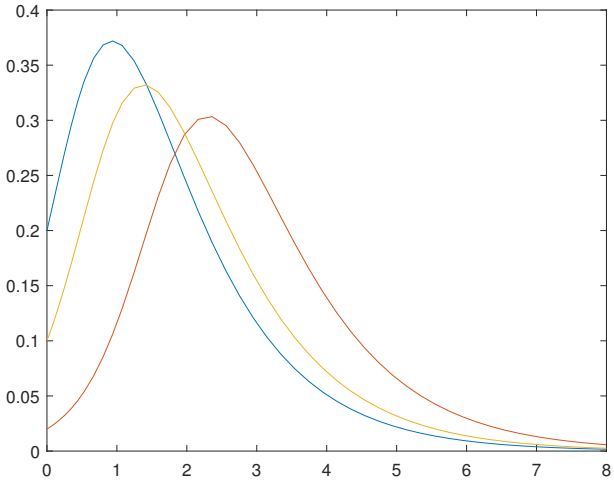

FIGURE 1. Infection levels in regions 1 (blue), 2 (red) and 3 (yellow), with confined regions ($m_{12} = m_{13} = 0$).

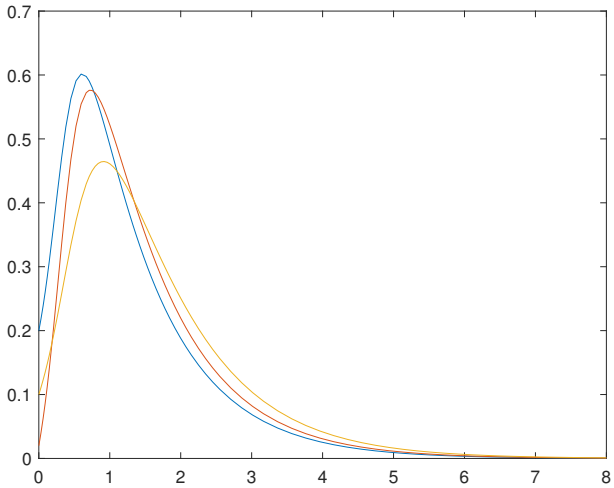

FIGURE 2. Infection levels in regions 1 (blue), 2 (red) and 3 (yellow), with strong interaction between regions and no flux limitation ($m_{12} = m_{13} = 1$, $K = 1000$).

Figure 2 describes the opposite situation, when all regions are allowed to interact freely. All three populations now exhibit much closer peaks. Even though A_2 and A_3 interact only through A_1, the evolution is almost identical in all three regions except for small times.

Figure 3 shows the result of favoring exchanges between A_1 and A_3, that are much more infected initially than A_2 ($m_{12} = 0.3$, $m_{13} = 1$). In this case, by taking K relatively large ($K = 3$), one also takes to some extent account their differences in infection as the epidemic progresses. The peaks are not as clustered, but are still close.

Figure 4 shows the result of favoring exchanges between A_1 and A_3 as before, ($m_{12} = 0.3, m_{13} = 1$), but giving now greater importance to the differences in infection levels ($K = 0.3$). The peaks are more separated.

Figure 4 shows the result of favoring exchanges between A_1 and A_3, with the same values of the m_{ij} ($m_{12} = 0.3$, $m_{13} = 1$), but giving greater importance to the differences in infection levels ($K = 0.3$). The infection peaks are more separated.

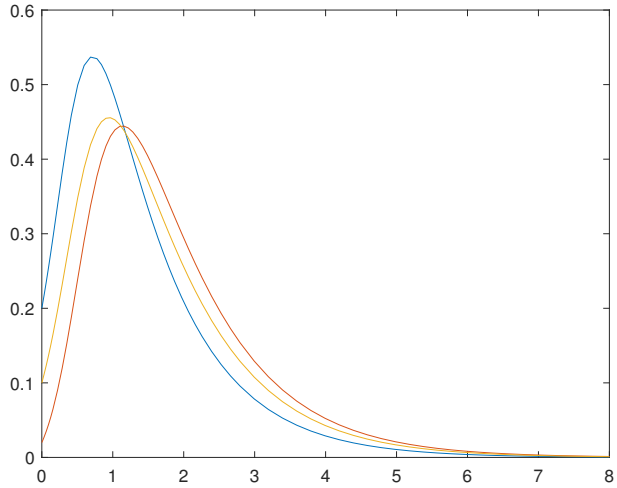

FIGURE 3. Infection levels in regions 1 (blue), 2 (red) and 3 (yellow), favoring exchanges between regions with similar levels of infection initially ($m_{12} = 0.3$, $m_{13} = 1$), with slight flux limitation ($K = 3$).

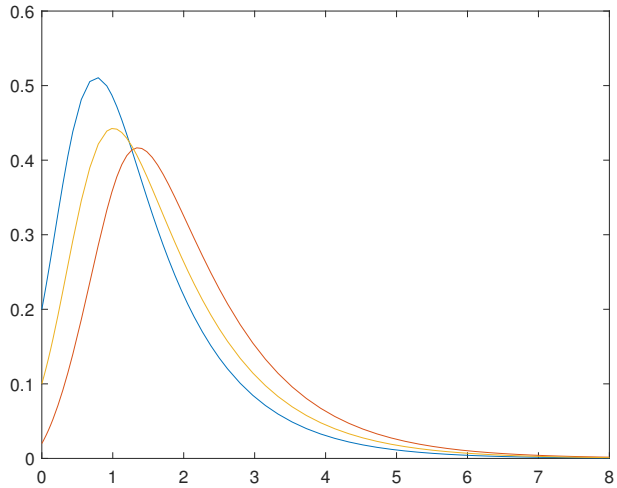

FIGURE 4. Infection levels in regions 1 (blue), 2 (red) and 3 (yellow), favoring exchanges between regions with similar levels of infection initially ($m_{12} = 0.3$, $m_{13} = 1$), with significant flux limitation ($K = 0.3$).

Figure 5 shows that, with the same values of m_{ij} but with a much larger effect of infection differences ($K = 0.0003$), the result is similar to the fully confined situation.

Figure 6 assumes $\beta = 1.6$, $\gamma = 1$, $m_{12} = m_{13} = 1$ and $K = 1000$ and $K = 0.03$ respectively. The separation of peaks is again apparent. In addition, a plateau formation is seen.

Figures 7 and 8 consider the effet of deconfinement through the linear increase of β. In Figure 7, β increases from 0.6 to 1.6, so that the reproduction had been significantly reduced by confinement, and does not increase very rapidly. The cases $K = 1000$ and $K = 0.003$ are presented. It is apparent that the introduction of restrictions on travel prevents weakens the "second wave" of infection after deconfinement, and separates the peaks.

In Figure 8, β increases from 0.8 to 3, so that the reproduction rate had only barely been pushed below 1 by confinement, and increases to higher values upon deconfinement. Even so, our method prevents the formation of a secondary wave

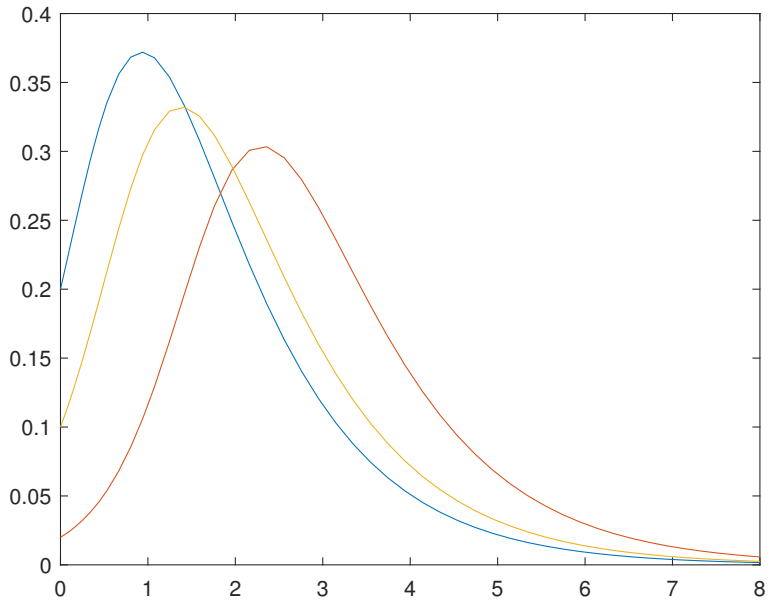

FIGURE 5. Infection levels in regions 1 (blue), 2 (red) and 3 (yellow), favoring exchanges between regions with similar levels of infection initially ($m_{12} = 0.3$, $m_{13} = 1$), with significant flux limitation ($K = 0.0003$).

immediately upon deconfinement. The peaks are considerably weaker with a small value of K.

We have discussed deconfinement strategies at the region level. Now, the SIR model does not distinguish, within a given region, infected individuals in or out of quarantine, nor susceptibles that are confined at home, as opposed to those that may move more freely (such as health workers for example). These are handled next, by introducing new compartments within regions.

3. Introduction of further compartment for confined classes

We introduce a slightly more elaborate model, involving quarantine as well as confined compartments. It is relevant for full confinement, or partial intra-regional deconfinement. It differs from earlier models by the splitting of the susceptible and infected classes into confined and unconfined ones, and by allowing a small, nonzero mobility to the confined classes, in accordance with what has been observed in recent weeks.

3.1. **Class I_Q.** We first write $I_i = F_i + Q_i$, distinguishing 'free' and 'quarantined' infectives. For simplicity, we did not distinguish exposed and symptomatic carriers; they are both treated as infected. We also assume that, even in times of confinement, there are unconfined classes, associated with food supplies or health workers.

We therefore need to distinguish subcompartments of confined and unconfined individuals, for each of the compartments except Q. Even F individuals can be confined (they cannot be distinguished from the S before testing). The confined individuals are characterized by having a much lower value of β (ideally zero, but this is not realistic). The confined are not quarantined, and may meet infectives while shopping etc. Let us write $S_i = S_{ic} + S_{iu}$, $F_i = F_{ic} + F_{iu}$, $R_i = R_{ic} + R_{iu}$, and $I_i = F_i + Q_i$.

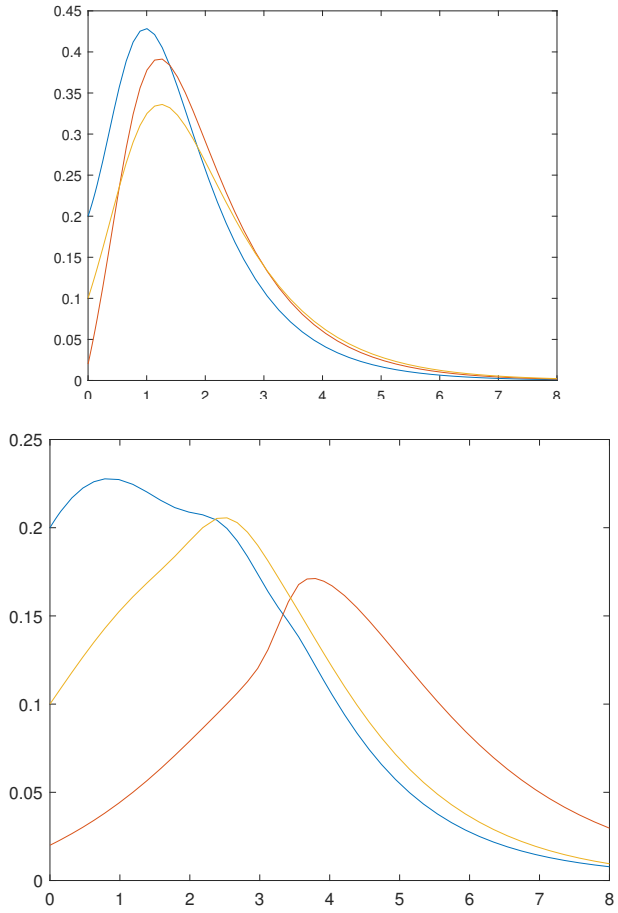

FIGURE 6. Infection levels in regions 1 (blue), 2 (red) and 3 (yellow), with $\beta = 1.6$, $\gamma = 1$, $m_{12} = m_{13} = 1$, $K = 1000$ (top) and $K = 0.03$ (bottom).

The introduction of mobility is very simple at this point: susceptibles in region A_i may not only meet the F_{iu} free infectives from their region, but also some from other regions A_j. Since the latter are not confined (since they can travel), it suffices to introduce terms of the form ι_i corresponding to the modified space-extended SIR model A or B discussed above, as follows. We also allow the susceptible to interact weakly with the confined infectives. The resulting equations are given next, and the new parameters it involves are discussed afterwards.

$$S'_{iu} = -\beta_i S_{iu}(F_{iu} + \iota_i)/N_i - \beta_c S_{iu} F_{ic}/N_i \tag{10}$$

$$S'_{ic} = -\beta_c S_{ic}(F_{iu} + \iota_i)/N_i - \sigma_c S_{ic} \tag{11}$$

$$F'_{iu} = \beta_c S_{iu}(F_{iu} + \iota_i)/N_i + \beta_c S_{iu} F_{ic}/N_i - \mu_i F_{iu} \tag{12}$$

$$F'_{ic} = \beta_c S_{ic}(F_{iu} + \iota_i)/N_i - \mu_i F_{ic} + \sigma_c F_{ic} \tag{13}$$

$$Q'_i = \mu_i F_i - (\gamma + d) Q_i \tag{14}$$

$$R'_{iu} = \gamma I_{iu}, \tag{15}$$

$$R'_{ic} = \gamma I_{ic}. \tag{16}$$

This relies on the following additional hypotheses

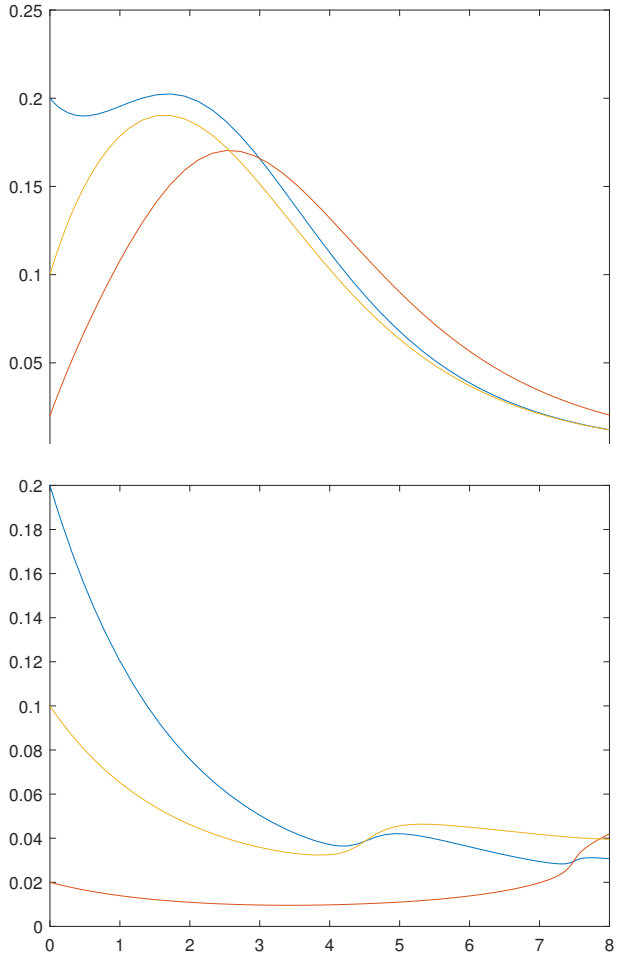

FIGURE 7. Infection levels in regions 1 (blue), 2 (red) and 3 (yellow), with β increasing from 0.6 to 1.6, $\gamma = 1$, $m_{12} = m_{13} = 1$, $K = 1000$ (top) and $K = 0.0003$ (bottom). The peaks in the bottom figure are weaker and remain apart.

(1) the unconfined susceptibles are mostly infected by asymptomatic carriers F from their own region and by infectives from other regions, but also through imperfect confinement ($\beta_c \ll \beta_i$, assumed independent of i);
(2) the quarantined do not contribute to the spreading of the disease;
(3) the confined susceptibles are infected not only by unconfined individuals, but also by the infectives confined with them, the latter effect being globally represented by the coefficient σ_c.
(4) the possibility that a confined person might infect another that is also confined, but in a different apartment or house, is neglected;
(5) the death rate of the F is neglected; so are deaths from other causes;
(6) free infected individuals develop symptoms at a constant rate μ_i (the subscript i leaves room for the possibility that the incubation period might depend on the environment in A_i, such as the average number of occupants in confined accomodation);
(7) all infected patients with symptoms are in quarantine (at home or in a hospital);
(8) births are neglected;
(9) there is no net population flux from one region to the other

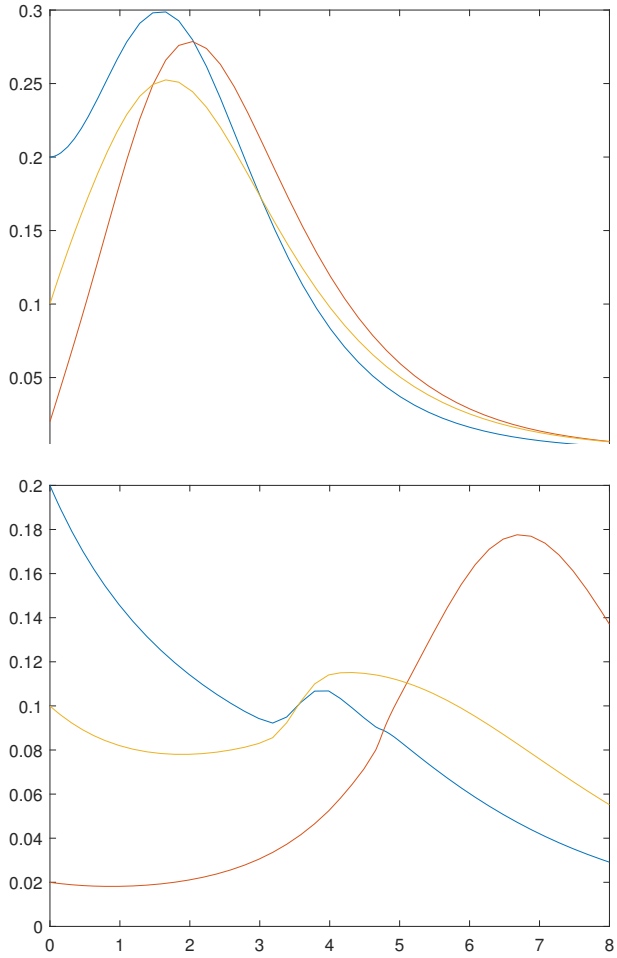

FIGURE 8. Infection levels in regions 1 (blue), 2 (red) and 3 (yellow), with β increasing from 0.6 to 1.6, $\gamma = 1$, $m_{12} = m_{13} = 1$, $K = 1000$ (top) and $K = 0.003$ (bottom). One observes delayed, weak secondary peaks in the bottom picture

4. Conclusion

We have proposed a modified space-extended SIR model containing restrictions on travel between regions, that favors communication between regions with a similar level of infection. We have proposed a model for confinement and deconfinement on this basis, in which public policies act by modifying the time dependence of the parameters in the model, representing new regulations as well as citizens' rational response to them.

Deconfinement amounts (i) to increasing in each region the value of β_c for the confined categories, representing the relaxing of lockdown within regions; (ii) increasing the parameters m and K representing selective restrictions on travel and (iii) restoring the terms ι_i representing allowed inter-regional travel or commuting to their pre-epidemic values by restoring the citizens' confidence that travel is safe. Confinement is the modification of the parameters in the opposite direction.

We have shown on examples that this model allows for communication between regions while avoiding that all regions should reach their peak at the same time, and may weaken significantly the secondary wave of infection consecutive to deconfinement.

It appears that the models proposed here are consistent with the current concepts in use in epidemiology, that should only be modified with care, since they are the outcome of the comparison of theory and observations for over a century (Serfling (1952), Hethcote (2000)). The class of models in this paper enables one to plan a progressive deconfinement, that can be controlled in real time according to the evolution of the disease, while avoiding excessive restrictions on citizens' freedom.

References

[1] Alex Arenas, Wesley Cota, Jesús Gómez-Gardeñes, Sergio Gómez, Clara Granell, Joan T. Matamalas, David Soriano and Benjamin Steinegger,"A mathematical model for the spatiotemporal epidemic spreading of COVID19," https://www.medrxiv.org/content/10.1101/2020.03.21.20040022v1.full.pdf

[2] Alex Arenas, Wesley Cota, Jesús Gómez-Gardeñes, Sergio Gómez, Clara Granell, Joan T. Matamalas, David Soriano and Benjamin Steinegger, "Derivation of the effective reproduction number R for COVID-19 in relation to mobility restrictions and confinement," https://www.medrxiv.org/content/10.1101/2020.04.06.20054320v1

[3] Samit Bhattacharyya and Timothy Reluga, "Game dynamic model of social distancing while cost of infection varies with epidemic burden," IMA Journal of Applied Mathematics (2019) **84**, 2343 doi:10.1093/imamat/hxy047

[4] Ottar N. Bjørnstad, Bryan T. Grenfell, Cecile Viboud, and Aaron A. King, "Comparison of alternative models of human movement and the spread of disease," http://dx.doi.org/10.1101/2019.12.19.882175

[5] M. Choisy, J.-F. Guégan and P. Rohani, "Mathematical Modeling of Infectious Diseases Dynamics," Chapter 22 of the Encyclopedia of Infectious Diseases: Modern Methodologies, (M.Tibayrenc, ed.), Wiley, 2007.

[6] Daniel T. Citron, Carlos A. Guerra, Andrew J. Dolgert, Sean L. Wu, John M. Henry, Héctor M. Sánchez and David L. Smith, "Comparing Metapopulation Dynamics of Infectious Diseases under Different Models ofHuman Movement," https://doi.org/10.1101/2020.04.05.20054304

[7] Herbert W. Hethcote, "The Mathematics of Infectious Diseases," SlAM Review, **42** : 4 (2000), 599-653.

[8] Matt J. Keeling and Bryan T. Grenfell, "Understanding the persistence of measles: reconciling theory, simulation and observation," Proc. of the Royal Society of London, B (2002) **269**, 335343.

[9] M. J. Keeling and J. V. Ross "On methods for studying stochastic disease dynamics," J. R. Soc. Interface **5**, (2008) 171181, https://dx.doi.org/10.1098/rsif.2007.1106

[10] W. O. Kermack, A. G. McKendrick, Contributions to the mathematical theory of epidemicsI. 1927. Bull. Math. Biol. 53, 3355 (1991).

[11] lun L. Lloyd, "Destabilization of epidemic models with the inclusion of realistic distributions of infectious periods," Proc. of the Royal Society of London, B (2001) **268**, 985-993.

[12] enjamin F. Maier and Dirk Brockmann, "Effective containment explains subexponential growth in recent confirmed COVID-19 cases in China," Science 10.1126/science.abb4557 (2020).

[13] k Shahid Nadim, Indrajit Ghosh, Joydev Chattopadhyay, "Short-term predictions and prevention strategies for COVID-2019: A model based study." https://arxiv.org/abs/2003.08150

[14] en Pei and Jeffrey Shaman (2020), "Initial Simulation of SARS-CoV2 Spread and Intervention Effects in the Continental US," https://doi.org/10.1101/2020.03.21.20040303

[15] obert E. Serfling, "Historical review of epidemic theory," Human Biology, Vol. 24, No. 3 (September, 1952), pp. 145-166

[16] ridip Sardar, Sk Shahid Nadim, Joydev Chattopadhyay, "Assessment of 21 Days Lockdown Effect in Some States and Overall India: A Predictive Mathematical Study on COVID-19 Outbreak." https://arxiv.org/abs/2004.03487

[17] oseph T Wu, Kathy Leung, Gabriel M Leung, "Nowcasting and forecasting the potential domestic and international spread of the 2019-nCoV outbreak originating in Wuhan, China: a modelling study," The Lancet, **395**, February 29, 2020, 689-697. https://www.thelancet.com/action/showPdf?pii=S0140-6736%2820%2930260-9

Université de Reims Champagne-Ardenne, Laboratoire de Mathématiques (CNRS, UMR 9008), Moulin de la Housse, B. P. 1039, F-51687 Reims, France
E-mail address: satyanad.kichenassamy@univ-reims.fr